Journal of Electromyography and Kinesiology 74 (2024) 102851

Contents lists available at ScienceDirect

Journal of Electromyography and Kinesiology

journal homepage: www.elsevier.com/locate/jelekin

Using force or EMG envelope as feedback signal for motor control system

M. Cogliati, A. Cudicio, C. Orizio *

Department of Clinical and Experimental Sciences, University of Brescia, Viale Europa, 11, 25123 Brescia, Italy

ARTICLE INFO

Keywords:
Neural feedback
Force feedback
Electromechanical coupling efficiency
Motor control

ABSTRACT

Purpose: This work studied muscle neuro-mechanics during symmetrical up-going ramp (UGR) and down-going ramp (DGR). Aim: to evaluate during the modulation of muscular action the outcome of force feedback (FF) or neural feedback (NF) on the behavior of the trailing signals - i.e. the EMG envelope (eEMG) for FF or force signal for NF.

Method: Subjects: 20. Investigated muscles: dorsal interosseous (FDI) and tibialis anterior (TA). Detected signals: force and EMG. Visual feedback: force (FF), eEMG (NF). Effort triangles: ramps duration 7.5 s, vertex at 50 and 100 % of the maximal voluntary action. Eventually, each subject performed FF50%, FF100%, NF50% and NF100% per each muscle. In each condition the areas beneath the force and eEMG signals were computed to calculate the ratios between the DGR and UGR values during the different tasks (force area DGR / force area UGR; eEMG area DGR / eEMG area UGR). Electro-mechanical coupling efficiency (EMCE) was estimated through the eEMG area / force area ratio for both UGR and DGR in each condition.

Results: a) FF. FDI: eEMG area ratio was 0.84 ± 0.15 and 0.73 ± 0.17 for FF50% and FF100%, respectively. TA: eEMG area ratio was 0.88 ± 0.11 and 0.91 ± 0.17 for FF50% and FF100%, respectively. b) NF: FDI: force area ratio was 1.18 ± 0.13 and 1.17 ± 0.13 for NF50% and NF100%, respectively. TA: force area ratio was 1.17 ± 0.21 and 1.07 ± 0.19 for NF50% and NF100%, respectively. c) DGR EMCE was greater than UGR EMCE in all four tasks.

Conclusion: The influence of UGR on deployed EMCE in the following force decrement phase underpins the changes of trailing signals area during DGR. This underlines the necessity of a careful evaluation of the features of FF or NF for experimental studies or rehabilitation purposes involving the motor control system.

1. Introduction

During daily life activities the central nervous system (CNS) doesn't control only the force production, but also its decrement. This means that the CNS must also have a specific strategy of motor units (MU) de-recruitment and of their discharge rate (DR) reduction aimed to precisely control the force decrease. However, this issue is poorly investigated, although some early needle EMG data suggested that there are changes in the recruitment state and/or DR of the different MU (de Luca et al., 1982) when the same level along the two subsequent - up-going and down-going – phases of a linearly varying triangular static torque effort is considered. More recently the described asymmetric DR behaviour has been confirmed using high density surface EMG from which the single motor unit contribution has been decomposed (Afsharipour et al., 2020).

In clinical setting as well as in kinesiological laboratories muscle neuromechanics is often investigated by means of bipolar global surface EMG. This signal encompasses the active MU action potentials (Basmajian and De Luca, 1985), as a consequence its thorough analysis may help in indirectly decoding some aspects of the MU activation/deactivation strategies adopted by the motor control system. Indeed, using global EMG in both large or small hand muscles, several studies provided data suggesting that the MU deactivation strategy does not simply mirror the activation one (Andrzejewska et al., 2014; Onushko et al., 2013; Orizio et al., 2010; Duchateau and Enoka, 2008; Kimura et al., 2003;). The obtained data suggest that with a force target that increases from a minimum to a maximum in a given time (up going ramp; UGR) and then decreases from maximum to minimum in the same interval (down going ramp; DGR) and with a torque signal that follows it with a minimal error, the EMG power is lower at the same torque value during DGR compared to UGR (Kimura et al., 2003; Orizio et al., 2010). This result suggests that during DGR a lower electrical activity from the active MU is needed and the efficiency of its conversion in mechanical output is improved. Data from electrically evoked contractions, applied

* Corresponding author at: Dept. Clinical and Experimental Sciences, University of Brescia, Viale Europa 11, 25123 Brescia, Italy.
E-mail address: claudio.orizio@unibs.it (C. Orizio).

https://doi.org/10.1016/j.jelekin.2023.102851
Received 12 May 2023; Received in revised form 30 October 2023; Accepted 28 November 2023
Available online 30 November 2023

both to single MU (Binder-Macleod and Clamann, 1989) or to the muscle main motor point (Orizio et al., 2013) clearly report a hysteretic behaviour of the mechanical output with more force during the descending phase of a frequency triangle stimulation train.

A way to quantify the changes in the EMG vs muscle mechanical activity during DGR vs UGR could be the calculation of the ratio between the force output per unit of myoelectrical activity, in both phases of the triangular effort, in order to define the so called electromechanical coupling efficiency (EMCE). EMCE has been defined by DeVries, (1968) and has been calculated using different mechanical counterparts of the electrical activity such as surface mechanomyogram (Akataki et al., 1996; Barry et al., 1990; Fukuhara et al., 2021; Lozano-García et al., 2021; Orizio et al., 1997) or force output (DeVries, 1968; Grosprêtre et al., 2018).

The above reported EMG-force relationship comes from experimental set-up based on triangular force feedback (FF) to the subject. The results may lead to the hypothesis that when forcing the neural drive to change in a triangular fashion, using the enveloped EMG as visual neural feedback (NF) to the subject, more force can be expected during the decontraction phase. This consideration can be of interest for neurorehabilitation or unilateral amputees training (in particular in "mirrored bilateral training" for subjects eligible for myoelectric prostheses (Mackay et al., 2023; Nielsen et al., 2011) when the neural function needs to be stimulated via biofeedback.

On these bases, the purpose of this experimental work is to verify whether the neural drive to the MU pool during triangular linearly varying muscle action is dependent on the different types of biofeedback – FF or NF - provided to the motor control system using a simple comparison between the muscle electrical activity (summarized by its envelope) and muscle mechanical output (converted in force signal by a load cell applied at the bone segment). The collected data could help in determining the specific scope of application of the force feedback or neural feedback in motor control performance enhancement. The calculation of the EMCE during UGR and DGR - when the two types of feedback will be provided to the subjects - will contribute to identify possible explanation to specific behaviours of electromechanical variables.

2. Methods

Twenty young (21.8 ± 2.26 years; 8 females and 12 males) without neurological or orthopaedic diseases, gave their informed consent to participate in the study after being given a full explanation of the experimental procedure according to the Declaration of Helsinki (1964) and its amends. The local Ethical Research Committee approved the proposed experimental design (CEIOC authorization: 17/2011).

2.1. Experimental set-up

The investigated muscles were the first dorsal interosseous (FDI) and the tibialis anterior (TA). The experimental set-up is reported in Fig. 1 for both FDI (panel A) and TA (panel B). The two muscles were chosen because their role in daily life activities and the importance in biofeedback training during functional recovery they may underwent.

For the FDI set-up the forearm of the subject was positioned halfway between pronation and supination in a custom designed brace and fixed, at the last three digits of the hand, by straps to the rigid frame. The index finger and thumb were at an angle of 90° and the tension during static abduction of the second digit was recorded through a load cell (SM-50 N, Interface Inc.; Scottsdale, Arizona, USA) coupled to the second phalanx (Cogliati et al., 2019). Given the adopted posture, the recorded tension was almost due to FDI activity.

For the TA set-up the dominant leg of participants was fixed in a specifically designed ergometer (Cogliati et al., 2023) equipped with a load cell to measure the applied tension during static tibialis anterior contraction. The hip angle was 90°, and the knee was fully extended (180°). The ankle was kept at its neutral angle (110°) (Cudicio et al., 2022). The foot was strapped to a wooden plate connected to a load cell (model SM-500 N, Interface Inc.; Scottsdale, Arizona, USA).

2.2. Procedure

The force signal was band-pass filtered 0–64 Hz and amplified by a MISO amplifier (OT Bioelettronica, Turin, Italy). The surface EMG signal was detected by two self-adhesive electrodes consisting of conductive metal discs (ϕ = 1 cm) previously covered with a conductive gel to minimize the contact impedance between the skin and the electrode itself. The self-adhesive 1 cm electrode diameter, commonly available in clinical setting and kinesiological laboratories, was chosen because it assures the possibility to detect a representative EMG from the muscle (Cavalcanti Garcia and Vieira, 2011; Vieira et al., 2011). The inter-electrode distance (IED) was 30 mm and 15 mm for TA and FDI, respectively.

According to Merletti and Cerone, (2020) once the superficial contour of the considered muscle was identified, the skin surface was rubbed with ethyl alcohol first (to remove the dead cells, oily substances

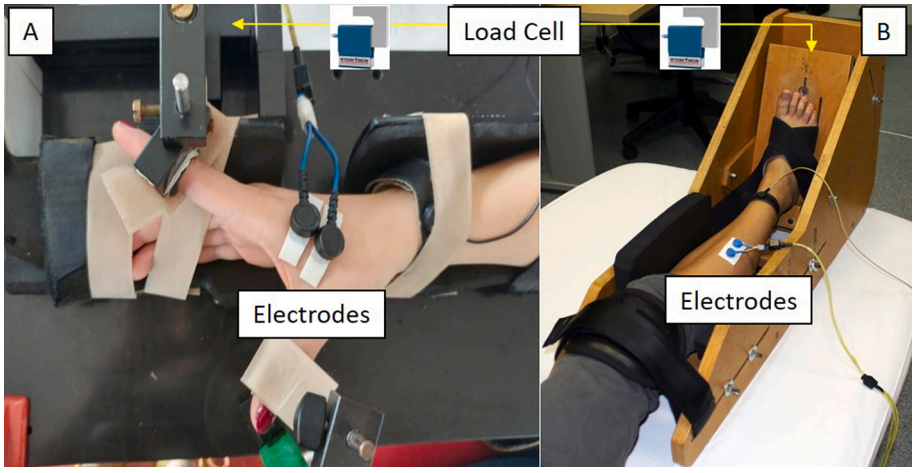

Fig. 1. Schematic representation of the experimental setup. Panel A: custom made ergometer for static tension recording during first dorsal interosseous muscle abduction in the vertical plane of the first digit. The relative position of the load cell and index finger is illustrated. Panel B: custom made ergometer for static tension recording during tibialis anterior muscle ankle dorsiflexion. The relative position of the wooden plate linked to the foot and the load cell is illustrated. Additionally, the EMG electrodes location over the muscles' belly has been reported.

and reduce the thickness of the stratum corneum) and then treated with abrasive conductive paste. Eventually two self-adhesive pre-jelled electrodes were applied on the muscle in the more distal portion of muscle surface toward its insertion. In particular, the electrodes were located beyond 51 % of the line between the anatomical landmark frames for TA (Barbero et al., 2012) and beyond 40 % of the muscle length for the FDI (Keenan et al., 2011). The values (51 % and 40 %) are meant from muscle origin. The electrodes were positioned with the inter-electrode axis parallel to the direction of the muscle fibers. The reference electrode was positioned on a non-electrical active area at the ankle or at the wrist of the subject to eliminate environmental interference. The signal was conditioned using a 10–512 Hz band-pass filter before being recorded. The bipolar surface EMG signals were detected using two out 16 available channels of the "EMG-16" amplifier (OT Bioelettronica, Turin, Italy). The EMG signals were also recorded as an enveloped signal (eEMG). A hardware enveloper, specially designed by OT Bioelettronica (Turin, Italy) was used. The instrument first rectified and then filtered (Butterworth 4th order, bandwidth 0–5.0 Hz) the detected EMG. The chosen band-with considered the cut-off frequencies that can be found in the literature (Torricelli et al., 2020).

The MVC was determined after the execution of three consecutive maximal efforts lasting 3 s, with 90 s interval in between. From the central 2 s of each effort the average of the force signal was calculated. The highest value was defined as MVC. In the same time period the average of the enveloped EMG was calculated. The resulting value was identified as the maximal enveloped EMG (MeEMG). As a consequence, during FF and NF the targets were presented as % of MVC and % of MeEMG, respectively.

The recordings from FDI and TA were randomly chosen and made in two different days one week apart. In each of the two days, once in the laboratory the subject was asked to familiarize with the triangular static contraction (0–50–0 % force at MVC, 0–100-0 % force at MVC, 0–50–0 % eEMG at MVC, 0–100-0 % eEMG at MVC) while a target was shown as a triangular red trajectory (see Fig. 2). As for the actual recordings the contractions always lasted 7.5 s for both the increasing and the decreasing phase of the static effort. The subject was asked to keep the exerted force signal or the eEMG as close as possible to the red lines on the screen (see Fig. 2). After familiarization the subject executed the four real linearly varying triangular contractions which signals were stored in a pc mass memory. Five minutes' rest were allowed between each contraction. The four tasks were characterised by different biofeedback (force feedback (FF) or neural feedback (NF) by the eEMG) and different highest levels (vertex of the triangles) of the requested muscle force or eEMG (50 % or 100 % of their value at MVC). As a consequence, each subject performed, in a random order, the tasks: FF50%, FF100%, NF50% and NF100%. During FF the force was the driving signal and the eEMG the trailing signal, vice versa during the NF trials (Fig. 2).

The force and the eEMG signals were sampled (1024 Hz) and stored on the PC hard disk using LabVIEW^{TM} software coupled with National Instruments DAQCard^{TM}. The same software was simultaneously providing the triangular target for FF and NF tasks.

2.3. Analysis

In Fig. 2 the description of the areas beneath the force signal and the eEMG – used for the following data analysis - are reported. For sake of clarity the dynamics of the force signal and eEMG are exemplified for two tasks (FF50% and NF50%). The areas beneath the force and eEMG have been calculated for both UGR (light grey) and DGR (dark grey). When the DGR/UGR Area Ratio is > 1 during DGR more force or eEMG

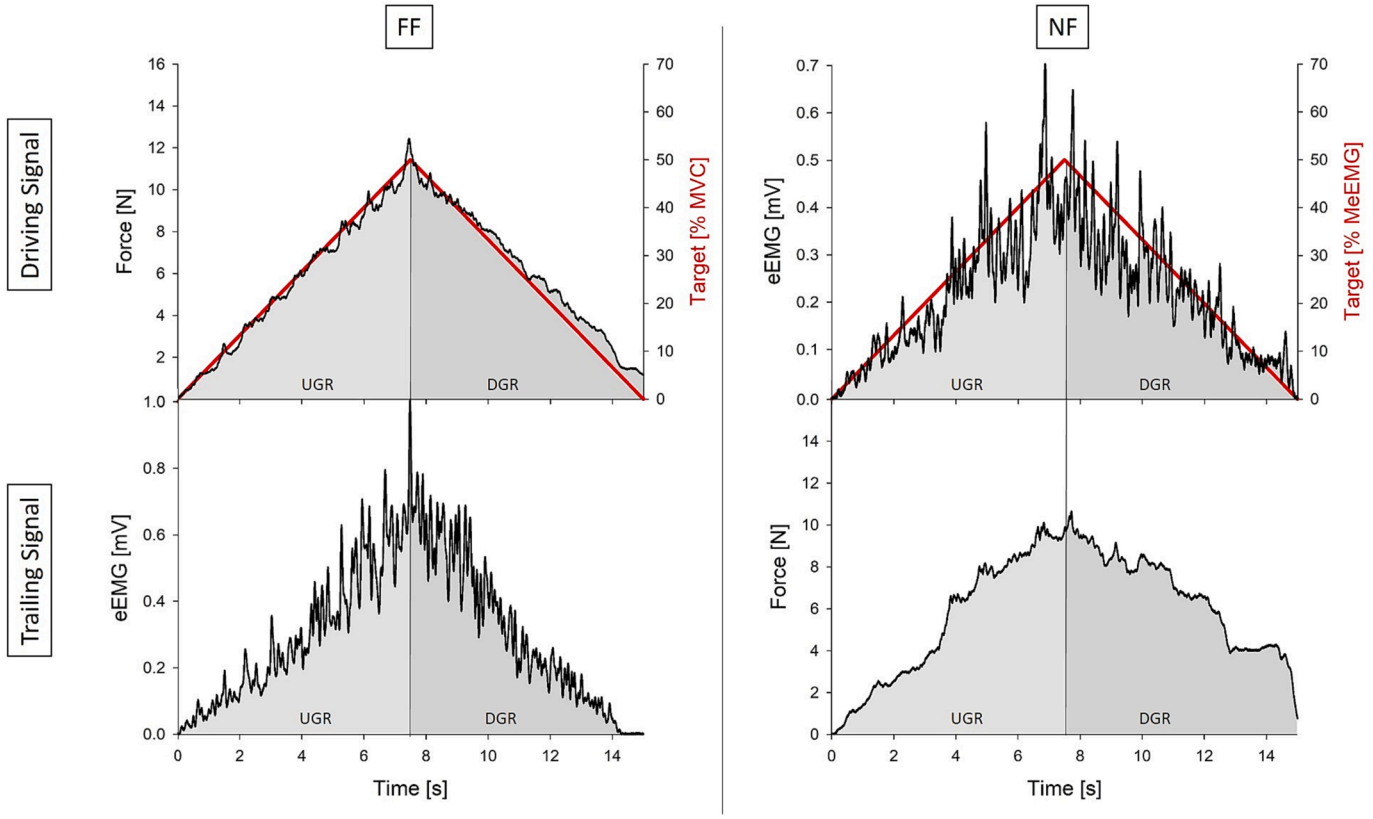

Fig. 2. Graphic representation of recorded signals (force and eEMG) during triangular FDI activity up to 50% MVC and 50% MeEMG as a response to FF and NF. Upper panels (driving signals): force and eEMG targets scaled to their values during MVC (red lines), actual force and eEMG (black lines). Lower panels (trailing signals): eEMG (on the lower left), force (on the lower right) produced by the corresponding trailing signal. Acronyms: MVC: maximal voluntary contraction; eEMG: enveloped EMG; MeEMG: maximal enveloped EMG). In light (UGR) and dark (DGR) grey the areas under the force or eEMG signals along the ramps are depicted. (For interpretation of the references to colour in this figure legend, the reader is referred to the web version of this article.)

is generated compared to UGR while opposite when the ratio is < 1. The same analysis was performed for FF and NF at 100 %MVC or MeEMG, respectively. To have an indication of the electro-mechanical coupling efficiency (EMCE) in the different phases of the linearly varying tasks, for each subject the ratio between the area beneath the force signal and eEMG of each triangular task (FF50%, FF100%, NF50% and NF100%) was computed separately during both UGR and DGR.

2.4. Statistical analysis

2.4.1. Force signal and eEMG DGR/UGR area Ratio

For each muscle a linear mixed-effect model (LMM) was applied as this statistical model accounts for the non-independence of observations. Specifically, random intercept models were applied with 'Type of biofeedback (FF or NF)', 'Intensity (50 % or 100 %)' and 'Analysed signal (Trailing or Driving)' as fixed effect and 'participant' as random effect (i.e., DGR/UGR Area Ratio ~ 1 + Type of feedback'* Intensity * Analysed signal' + (1 | participant)). LMM was implemented using the package *lmerTest* (Kuznetsova et al., 2017) with the Kenward-Roger's method to approximate the degrees of freedom and estimate the p-values. The *emmeans* package was used to determine estimated marginal means and their differences with 95 % confidence intervals. The cut-off for statistical significance was set at $p < 0.05$. The effect size was estimated by calculating Cohen's d parameter. The analysis was performed using RStudio 2022.12.0 + 353 "Elsbeth Geranium" Release.

2.4.2. EMCE

The seek for the possible differences between the EMCE during DGR and UGR the same LMM approach was used for each muscle. The analysis included 'Type of biofeedback (FF or NF)', 'Intensity (50 % or 100 %)' and the phase of the triangular effort (UGR or DGR)'' as fixed effect and 'participant' as random effect (i.e., DGR/UGR Area Ratio ~ 1 + Type of feedback'* Intensity * phase of the triangular effort' + (1 | participant)).

3. Results

The voluntary maximal effort provided 28.28 ± 8.61 N and 0.1 ± 0.03 mV (FDI) or 172.51 ± 52.75 N and 0.2 ± 0.09 mV (TA) for force and eEMG, respectively.

3.1. DGR/UGR area ratio

The results of the group analysis for FDI are presented in Fig. 3. The LMM revealed a significant effect of the type of biofeedback on the DGR/UGR Area Ratio ($p = 0.031$), but no significant effects were observed for intensity ($p = 0.190$) or analysed signal ($p = 0.309$). An interaction between the three factors was also observed ($p = 0.032$). Specifically, when the trailing signal was considered, the DGR/UGR Area Ratio was found to be lower in the FF condition compared to the NF condition for both 50 % (Kenward-Roger's method, $p < 0.0001$; Cohen's $d = 2.38$; CI: [1.75—–3.01]) and 100 % (Kenward-Roger's method, $p < 0.0001$; Cohen's $d = 3.19$; CI: [2.56—–3.83]).

Fig. 4 presents the group analysis results for TA. The LMM revealed a significant effect of the type of biofeedback on the DGR/UGR Area Ratio ($p < 0.001$), while no significant effects were found for intensity ($p = 0.205$) or analysed signal ($p = 0.775$). There was no significant interaction between these three factors ($p = 0.360$). When the trailing signal was taken into consideration, the DGR/UGR Area Ratio was found to be lower in the FF condition compared to the NF condition for 50 % (Kenward-Roger's method, $p < 0.0001$, Cohen's $d = 2.22$; CI: [1.60 – 2.85]) and 100 % (Kenward-Roger's method, $p = 0.009$, Cohen's $d = 1.16$; CI: [0.54—–1.79]).

In conclusion, the application of force as biofeedback resulted in a smaller area under the eEMG signal for DGR compared to UGR. Conversely, when using eEMG as biofeedback, the area under the force signal for the DGR was larger than in the UGR. As expected, no significant differences were observed in the DGR/UGR Area Ratio derived from the driving signals when comparing data from FF and NF ($p = 1.000$). Similarly, the DGR/UGR Area Ratio obtained from the trailing signals showed no significant differences ($p = 1.000$) when comparing data from 50 % and 100 % in both FF and NF conditions.

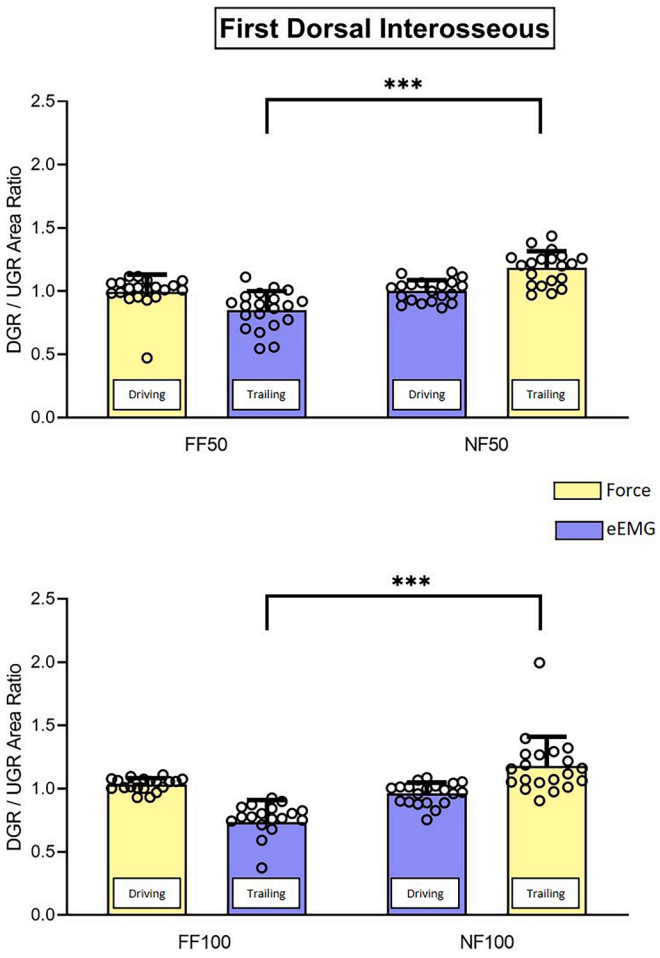

Fig. 3. Analysis of DGR/UGR Area Ratio for FDI. The plot displays the mean and standard deviation of the DGR/UGR Area Ratio at two different levels: 50 % (upper panel) and 100 % (lower panel) of MVC. The colors yellow and blue represent the area ratio of force and eEMG signal, respectively. The statistical differences between the area ratio of trailing signals obtained during FF and NF are indicated by asterisks [$p < 0.05$ (*); $p < 0.01$ (**); $p < 0.001$ (***)]. The individual subject values are displayed using empty dots. Acronyms: eEMG: enveloped EMG; UGR: up-going ramp; DGR: down-going ramp; FF50: force feedback at 50 % of the maximal isometric effort; NF50: enveloped EMG feedback at 50 % of the maximal isometric effort; FF100: force feedback at 100 % of the maximal isometric effort; NF100: enveloped EMG feedback at 100 % of the maximal isometric effort). (For interpretation of the references to colour in this figure legend, the reader is referred to the web version of this article.)

3.2. EMCE

The results of the group analysis for FDI and TA are presented in Fig. 5. For FDI, the LMM analysis revealed no significant effect for the phase of the triangular effort ($p = 0.484$), intensity ($p = 0.284$), or type of feedback ($p = 0.701$). However, there was a significant interaction between these three factors ($p = 0.050$). Specifically, for the FF task, the EMCE was found to be lower in the UGR compared to the DGR for both 50 % (Kenward-Roger's method, $p = 0.0019$; Cohen's $d = 1.30$; CI: [0.67 – 1.92]) and 100 % (Kenward-Roger's method, $p < 0.0001$, Cohen's $d = 2.75$; CI: [2.11—–3.39]). Similarly, for the NF task, the EMCE was found

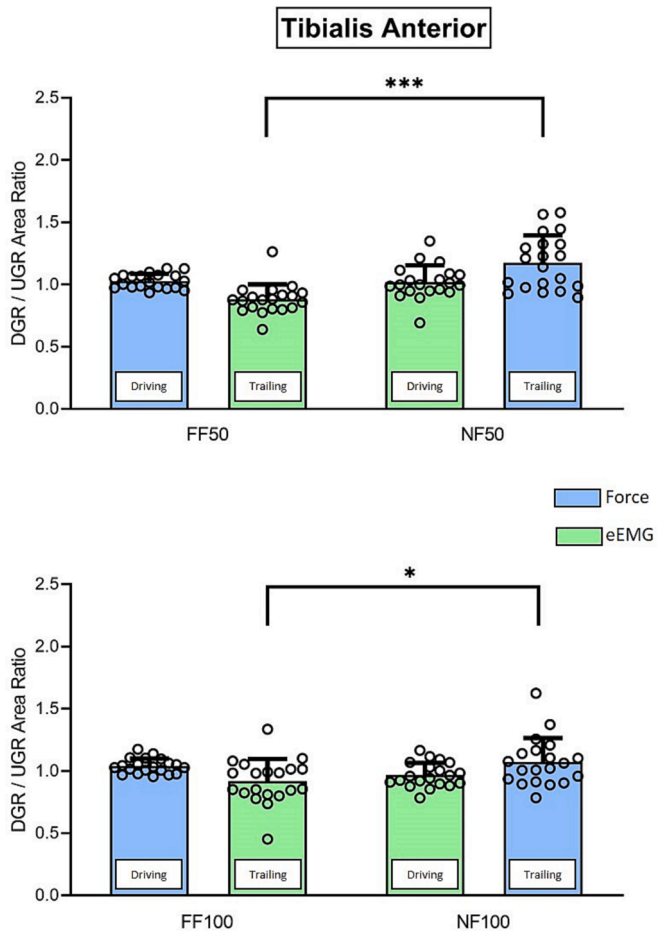

Fig. 4. Analysis of DGR/UGR Area Ratio for TA. The plot displays the mean and standard deviation of the DGR/UGR Area Ratio at two different levels: 50 % (upper panel) and 100 % (lower panel) of MVC. The colors light blue and green represent the area ratio of force and eEMG signal, respectively. The statistical differences between the area ratio of trailing signals obtained during FF and NF are indicated by asterisks [$p < 0.05$ (*); $p < 0.01$ (**); $p < 0.001$ (***)]. The individual subject values are displayed using empty dots. Acronyms: eEMG: enveloped EMG; UGR: up-going ramp; DGR: down-going ramp; FF50: force feedback at 50 % of the maximal isometric effort; NF50: enveloped EMG feedback at 50 % of the maximal isometric effort; FF100: force feedback at 100 % of the maximal isometric effort; NF100: enveloped EMG feedback at 100 % of the maximal isometric effort). (For interpretation of the references to colour in this figure legend, the reader is referred to the web version of this article.)

to be lower in the UGR compared to the DGR for both 50 % (Kenward-Roger's method, $p = 0.026$; Cohen's $d = 1.07$; CI: [0.44 – 1.69]) and 100 % (Kenward-Roger's method, $p = 0.0024$; Cohen's $d = 1.28$; CI: [0.65 – 1.90]).

The LMM analysis revealed that for TA, there was a significant effect for the phase of the triangular effort on the EMCE ($p = 0.0001$), but no significant effects were observed for intensity ($p = 0.755$) or type of feedback ($p = 0.989$). There was no significant interaction between these three factors ($p = 0.460$). Specifically, for the FF task, the EMCE was found to be lower in the UGR compared to the DGR for both 50 % (Kenward-Roger's method, $p < 0.0001$; Cohen's $d = 1.88$; CI: [1.26—2.51]) and 100 % (Kenward-Roger's method, $p < 0.0001$; Cohen's $d = 1.86$; CI: [1.22 – 2.51]). Similarly, for the NF task, the EMCE was found to be lower in the UGR compared to the DGR for both 50 % (Kenward-Roger's method, $p = 0.0001$; Cohen's $d = 1.56$; CI: [0.94 – 2.19]) and 100 % (Kenward-Roger's method, $p = 0.024$; Cohen's $d = 1.07$; CI: [0.45 – 1.70]).

4. Discussion

This study for the first time quantifies - during triangular linearly varying neural drive provided by eEMG feedback signal - the extra force produced during the de-contraction phase. Moreover, it resulted that the MU activation/deactivation strategies are biofeedback sensitive changing if this last is the mechanical signal (FF) or eEMG (NF). These results seem to be related to the electromechanical coupling efficiency increase during DGR induced by a previous UGR.

4.1. Force feedback

The force signal is commonly used as a biofeedback to study motor control system features in different conditions, in particular when static contractions are under study (Afsharipour et al., 2020; Cogliati et al., 2019; Jesunathadas et al., 2010; Kimura et al., 2003; Orizio et al., 2010). Previous works suggested that during voluntary contractions, when the muscle tension is gradually varying in two adjoining up and down going phases, the surface EMG parameters, monitoring the neural drive to the motoneuronal pool and its excitability, present specific behaviors. Orizio et al. (2010) reported a lower EMG root mean square value during DGR compared to UGR when the same effort level is considered. The authors suggested that motor control system may reduce the number and the firing rate of the active motor units (MU) contributing to the EMG generation. Several determinants can be considered: a) a lower motoneuronal excitability during rapid relaxation phase from steady contraction compared to the rest condition (Schieppati et al., 1986; Schieppati and Crenna, 1985); b) a clear hysteresis of the corticospinal excitability along a triangular static tension production resulting in a greater motor evoked potential, elicited by transcranial magnetic stimulation, during the whole period of UGR compared to DGR (Kimura et al., 2003); c) a different behavior, shifted toward lower values, of the MU firing rate and total exerted force relationship during linear relaxation after linear contraction (Denier van der Gon et al., 1985); d) an evident sag of the MU firing rate from the beginning of the relaxation phase of a force triangular task that is not recovered during the relaxation time determining a lower FR along the whole phase (Afsharipour et al., 2020). Given that FR is strongly influencing the EMG time domain variables (Christie et al., 2009) the results from the works of Denier van der Gon et al. (1985) and Afsharipour et al. (2020) may contribute to explain the evident smaller EMG activity during DGR in first dorsal interosseous linearly varying tension (Orizio et al., 2010). According to Kimura et al. (2003) the determinants of the above reported changes in the functional features of the motor control involved structures, which can be tracked through the surface EMG analysis, should include also the peripheral increase of the motor units' mechanical efficiency acquired during the up-going contraction phase later deployed during the relaxation. Indeed, the potentiating influence of the UGR on the motor units mechanical output was already described since early'80 s (De Luca et al., 1982). Eventually, the more efficient tension development during "relaxation might require relatively lower muscle activation for a similar level of tension development during muscle contraction" (Kimura et al., 2003).

Finally, the results of the FF protocol confirm the literature data and suggest that when the experimental procedure is aimed to investigate the outcomes of a symmetrical linear variation of the neural drive the use of the force signal as an input to the motor control system may not be the most suitable tool for the purpose.

4.2. Neural feedback

It is well known that modifications of the neural drive to the muscle determines improvement in its muscle mechanical output (Moritani and DeVries, 1980). As a consequence, NF has been purposely used to modulate motor learning of new synergies between muscle (Torricelli et al., 2020), re-learning of muscle sub-maximal activation motor

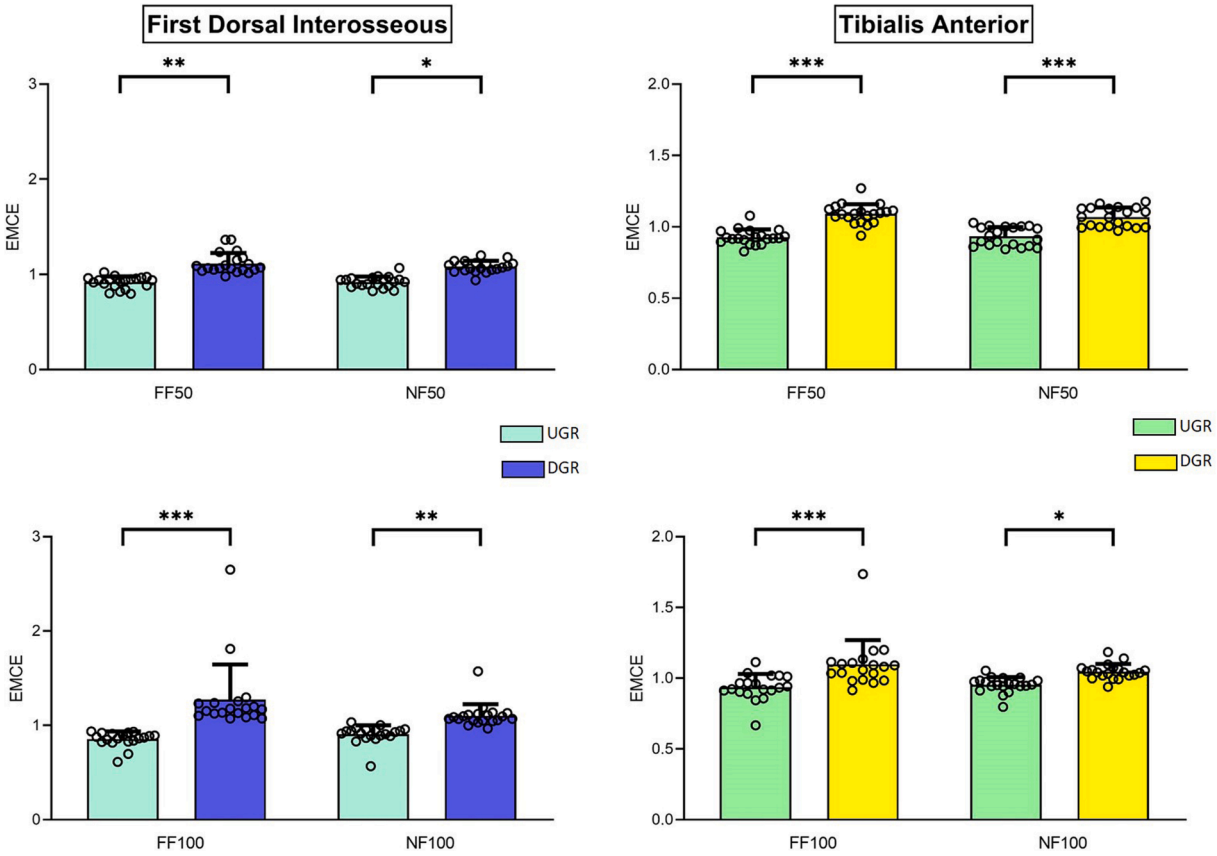

Fig. 5. Analysis of EMCE for FDI and TA. The plot displays the mean and standard deviation of the EMCE at two different levels: 50 % (upper panel) and 100 % (lower panel) of MVC. The FDI results are summarized in the left panels. The TA results are summarized in the right panels. The light blue and light green colors represent the EMCE during up-going-ramp (UGR), while blue and yellow colors represent the EMCE during down-going-ramp (DGR). The statistical differences between UGR and DGR during FF and NF are indicated by asterisks [$p < 0.05$ (*); $p < 0.01$ (**); $p < 0.001$ (***)]. The individual subject values are displayed using empty dots. Acronyms: EMCE: electro-mechanical coupling efficiency; eEMG: UGR: up-going ramp; DGR: down-going ramp; FF50: force feedback at 50 % of the maximal isometric effort; NF50: enveloped EMG feedback at 50 % of the maximal isometric effort; FF100: force feedback at 100 % of the maximal isometric effort; NF100: enveloped EMG feedback at 100 % of the maximal isometric effort). (For interpretation of the references to colour in this figure legend, the reader is referred to the web version of this article.)

control after musculoskeletal injuries (Kirnap et al., 2005), improvement of muscle force output during maximal volitional action (Ekblom and Eriksson, 2012; Mackay et al., 2023) and also as an indirect tool for force estimation technique (Staudenmann et al., 2010). In this study NF provided a symmetrical triangular eEMG as an input to the motor control system leading to a symmetrical neural drive to the motor units pool. A similar symmetrical triangular neural drive can be provided using neuromuscular stimulation.

Indeed, Orizio et al., 2013 reported that, even in the human muscles stimulated at the motor point, both a triangular change of the tetanic train amplitude (modulating the MU recruitment level) or of the maximal stimulus frequency (modulating the force output along the force/frequency curve) determined a clear positive hysteresis with an extra-force during the DGR compared to the UGR. The two different stimulation patterns were supposed to mimic the modulation of the two means (Recruitment and DR) that the CNS uses to modify the level of force produced by a muscle. These results from humans are in agreement with data from animal motor units obtained using an increasing/decreasing frequency (Binder-Macleod and Clamann, 1989; Łochyński and Celichowski, 2009) or changing through the time the number of the active cooperating motor unit motor units (Clamann and Schelhorn, 1988). The cited papers collectively underline the important role of the visco-elastic components of the muscle model in providing more tension during the DGR. They can contribute to explain the DGR extra-force reported during NF task.

4.3. FDI and TA response to FF and NF

It is well known that TA can recruits motor units up to 70 % MVC (Del Vecchio et al., 2018) while FDI completes recruitment at 40 % MVC (de Luca et al., 1982; Seki and Narusawa, 1996) and within 10 % MVC already engages half of its motor units (de Luca et al., 1982; Milner-Brown et al., 1973). It is important to note that during FF50 and NF50 the triangular ramps we administered presented a maximal value corresponding to the 50 % of the muscle force generation capacity at which the MU recruitment was incomplete in TA while already complete in FDI which uses, in the last part of the ramp, the increment of the global MU firing rate to achieve the highest requested tension levels. It seems evident that the extra-force produced during the DGR is present in NF data independently from the motor unit activation pattern the muscle adopted during the previous UGR.

4.4. Different amplitude and speed of variation of the triangular effort and EMCE during UGR and DGR

The two triangular patterns used in this study (0–50-0 % or 0–100-0 % of the MVC for both FF and NF) were asking the subjects to produce different levels of maximal activity, with two different velocities of the force or eEMG changes (6.6 %/s and 13.3 %/s, respectively) along the two lines of the triangle. Our results suggest that the lowering of eEMG activity (FF task) as well as the extra-force (NF task) during DGR compared to UGR are detectable in both high-fast and low-slow target

triangles. Moreover, the amount of the changes is similar. It can be concluded that increasing the maximal value of the requested maximal activity and its rate of production during UGR above 50 % and 6.6 %/s, respectively, does not further modify the mechanical response, during DGR, of the viscoelastic components to the previous increment of muscular activation.

How the non-symmetrical behaviour of the trailing signal (DGR reduced EMG and extra-force during FF and NF, respectively) can be explained? A factor that can influence our main results is the EMCE increment due to the previous UGR. Out of the feedback used during the first part of the triangle the increase of the requested level of activity determines that more tension is produced per each mV of electrical activity during DGR. Also in this case the increase in EMCE takes place independently from the triangle features (height and rate) of the targeted linearly varying effort.

In addition to MU potentiation suggested by de Luca et al., (1982) the mechanical hysteresis during DGR may contribute to additional muscle output tension during relaxation through the changes in the elastic properties of acto-myosin cross-bridges loaded in the previous UGR (Kimura et al., 2003). As a consequence it may be concluded with Frigon et al., (2011) that the extra-torque during muscle de-tensioning may be mediated by an intrinsic muscle property with no need for CNS involvement. This interpretation is supported by the data from Orizio et al. (2013) in which the neural drive was completely controlled by the electrical triangular stimulation (for amplitude and frequency) with no involvement of the CNS. The importance of the peripheral origin of the muscle extra-force during the deactivation phase was pointed out already in the 1998 by Baratta et al. They clearly reported that when stimulating a muscle changing in a triangular fashion the stimuli amplitude, the force during the DGR mirrored the values presented during UGR only if it was also provided as a feed-back signal to the external controller driving the stimulator.

4.5. Critique of the methods, limitations and possible perspective

Several recent methodological papers (Besomi et al., 2020, 2019; McManus et al., 2021; Merletti and Muceli, 2019) provide data about the properties of the surface EMG detection system able to minimize the signal frequency content filtering. In particular Merletti and Muceli, (2019) suggested that electrodes diameter should be ≤ 5 mm (for metal discs) with IED ≤ 10 mm. According to these indications the detected EMG should be highly reliable for single motor unit activity identification - after high density surface EMG decomposition - as well as for precise estimation of specific time and frequency domain EMG parameters. In our study the surface EMG was recorded in order to have a signal able to reflect the global neural drive to the muscle to be compared with the global mechanical generated force. With this in mind, specific indications from the literature on the topic cannot be disregarded. Indeed, Vieira et al., (2017) demonstrated that the EMG signal amplitude (estimated by RMS) increased up to about 3.7 and 4 cm IEDs for soleus and gastrocnemius, respectively. These IEDs leads to the detection of "a more representative and thus reliable recording" of muscle activity. Recently (Vieira et al., 2023) reported that the greater the IED the more sensitive the bipolar EMG is to the joint torque changes and that in order to correctly detect the EMG onset earlier than the torque onset - with an indication of the electromechanical delay − 30 mm IED is recommended in large muscles. On the contrary short IEDs may result "in EMG descriptors of dubious physiological validity" (Vieira et al., 2023). Moreover, dos Anjos et al., (2022) - to provide an appropriate biofeedback to the subject related to the activity of the "most of the fibers of the targeted muscles" - used electrodes with a diameter of 2.4 cm and 3.5 cm IED. On these bases the electrode dimensions and IED used in this work may be considered suitable for an accurate investigation of the mechanical output and neural drive relationship when FF or NF were provided to the subjects.

Within the limitations of the study it has to be considered the lack of a sufficiently wide sample of participants that did not allow comparison between genders. Since motor control drive may vary between males and females because specific functional properties of the involved neural structures (Jenz et al., 2023) it is important to conduct further research that includes a representative sample of both genders to gain a more comprehensive understanding of the potential differences in response to the motor control system acting through FF or NF. Another limitation is related to the impossibility to link the specific force output vs muscle neural drive – during FF or NF – to changes in MU activation-deactivation patterns. Future studies with high density surface EMG will possibly contribute to get some direct insights about the different motor control system adopted MU activation/deactivation strategies according to FF or NF tasks. Furthermore, we compared data from the entire UGR and DGR. Indeed, important information could be drawn from specific force intervals where slow and fast MUs as well as only slow MUs were active. Indeed, in the last condition the potentiation effect of UGR on slow twitch motor units could be better investigated (de Luca et al., 1982).

5. Conclusions

1. Force feedback is suitable for training of mechanical output accuracy even during force decrement control. EMG envelope feedback is crucial when dynamic symmetrical neural drive to MU pool training is the goal (such as for training of unilateral amputees eligible for myoelectric prostheses or rehabilitation protocols aimed to improve the fine motor control).
2. The triangular FF during voluntary static contraction may not be the most appropriate input to the motor system when the motoneuronal excitability is under investigation and a symmetrical motor drive is needed.
3. Data from NF recordings suggest that when the eEMG is used as a biofeedback an extra force is produced during the DGR, on the contrary when FF is used a lower eEMG, i.e. a lower neural drive, is present during the DGR. It can be concluded that, independently from the feedback type, the relationship between the neural drive level and the muscle mechanical output, is never symmetrical in the two phases (UGR-DGR).
4. The greater EMCE during the force decremental phase, caused by previous muscle increasing activity, can be one of the factors playing an important role in non-symmetrical behavior of the trailing signals when a linearly varying up-going/down-going static effort is considered.

Declaration of competing interest

The authors declare that they have no known competing financial interests or personal relationships that could have appeared to influence the work reported in this paper.

Acknowledgements

The Authors thank Professor Francesco Negro for his help in focusing the issues of the work conceptualization, Doctor Helio da Veiga Cabral for his help in identification of the most suitable statistical tool for data analysis and the subjects that agreed to participate in the study.

References

Afsharipour, B., Manzur, N., Duchcherer, J., Fenrich, K.F., Thompson, C.K., Negro, F., Quinlan, K.A., Bennett, D.J., Gorassini, M.A., 2020. Estimation of self-sustained activity produced by persistent inward currents using firing rate profiles of multiple motor units in humans. J. Neurophysiol. 124, 63–85. https://doi.org/10.1152/jn.00194.2020.

Akataki, K., Mita, K., Itoh, K., Suzuki, N., Watakabe, M., 1996. Acoustic and electrical activities during voluntary isometric contraction of biceps brachii muscles in patients with spastic cerebral palsy. Muscle Nerve 19, 1252–1257. https://doi.org/10.1002/(SICI)1097-4598(199610)19:10<1252::AID-MUS2>3.0.CO;2-D.

Andrzejewska, R., Jaskólski, A., Jaskólska, A., Gobbo, M., Orizio, C., 2014. Electromyogram features during linear torque decrement and their changes with fatigue. Eur. J. Appl. Physiol. 114, 2105–2117. https://doi.org/10.1007/s00421-014-2928-4.

Baratta, R.V., Zhou, B.H., Solomonow, M., D'Ambrosia, R.D., 1998. Force feedback control of motor unit recruitment in isometric muscle. J. Biomech. 31, 469–478. https://doi.org/10.1016/S0021-9290(98)00042-6.

Barbero, M., Merletti, R., Rainoldi, A., Barbero, M., Merletti, R., Rainoldi, A., 2012. Introduction and Applications of Surface EMG, in: Atlas of Muscle Innervation Zones. https://doi.org/10.1007/978-88-470-2463-2_1.

Barry, D.T., Gordon, K.E., Hinton, G.G., 1990. Acoustic and surface EMG diagnosis of pediatric muscle disease. Muscle Nerve 13, 286–290. https://doi.org/10.1002/MUS.880130403.

Basmajian, J.V., De Luca, C.J., 1985. Muscles alive : their functions revealed by electromyography. Muscles Alive Their Funct. Reveal. by Electromyogr. 65–100.

Besomi, M., Hodges, P.W., Van Dieën, J., Carson, R.G., Clancy, E.A., Disselhorst-Klug, C., Holobar, A., Hug, F., Kiernan, M.C., Lowery, M., McGill, K., Merletti, R., Perreault, E., Søgaard, K., Tucker, K., Besier, T., Enoka, R., Falla, D., Farina, D., Gandevia, S., Rothwell, J.C., Vicenzino, B., Wrigley, T., 2019. Consensus for experimental design in electromyography (CEDE) project: Electrode selection matrix. J. Electromyogr. Kinesiol. 48, 128–144. https://doi.org/10.1016/j.jelekin.2019.07.008.

Besomi, M., Hodges, P.W., Clancy, E.A., Van Dieën, J., Hug, F., Lowery, M., Merletti, R., Søgaard, K., Wrigley, T., Besier, T., Carson, R.G., Disselhorst-Klug, C., Enoka, R.M., Falla, D., Farina, D., Gandevia, S., Holobar, A., Kiernan, M.C., McGill, K., Perreault, E., Rothwell, J.C., Tucker, K., 2020. Consensus for experimental design in electromyography (CEDE) project: Amplitude normalization matrix. J. Electromyogr. Kinesiol. 53, 102438 https://doi.org/10.1016/j.jelekin.2020.102438.

Binder-Macleod, S.A., Clamann, H.P., 1989. Force output of cat motor units stimulated with trains of linearly varying frequency. J. Neurophysiol. 61, 208–217. https://doi.org/10.1152/jn.1989.61.1.208.

Cavalcanti Garcia, M.A., Vieira, T.M.M., 2011. Surface electromyography: Why, when and how to use it. R e v i s t a A n d a l u z a d e Med. Del Deport. 4, 17–28.

Christie, A., Greig Inglis, · J, Kamen, G., Gabriel, D.A., 2009. Relationships between surface EMG variables and motor unit Wring rates. Eur J Appl Physiol 107, 177–185. https://doi.org/10.1007/s00421-009-1113-7.

Clamann, H.P., Schelhorn, T.B., 1988. Nonlinear force addition of newly recruited motor units in the cat hindlimb. Muscle Nerve 11, 1079–1089. https://doi.org/10.1002/MUS.880111012.

Cogliati, M., Cudicio, A., Negro, F., Gaffurini, P., Bissolotti, L.M., Orizio, C., 2019. Influence of age on motor control accuracy during static ramp contractions. Exp. Brain Res. 237 (8), 1889–1897.

Cogliati, M., Cudicio, A., Benedini, M., Cabral, H.V., Negro, F., Reggiani, C., Orizio, C., 2023. Influence of age on force and re-lengthening dynamics after tetanic stimulation withdrawal in the tibialis anterior muscle. Eur. J. Appl. Physiol. 123 (8), 1825–1836.

Cudicio, A., Martinez-Valdes, E., Cogliati, M., Orizio, C., Negro, F., 2022. The force-generation capacity of the tibialis anterior muscle at different muscle-tendon lengths depends on its motor unit contractile properties. Eur. J. Appl. Physiol. 122, 317–330. https://doi.org/10.1007/s00421-021-04829-8.

de Luca, C.J., LeFever, R.S., McCue, M.P., Xenakis, A.P., 1982. Behaviour of human motor units in different muscles during linearly varying contractions. J. Physiol. 329, 113–128. https://doi.org/10.1113/jphysiol.1982.sp014293.

Del Vecchio, A., Negro, F., Felici, F., Farina, D., 2018. Distribution of muscle fibre conduction velocity for representative samples of motor units in the full recruitment range of the tibialis anterior muscle. Acta Physiol. 222 https://doi.org/10.1111/apha.12930.

Denier van der Gon, J.J., ter Haar Romeny, B.M., van Zuylen, E.J., 1985. Behaviour of motor units of human arm muscles: differences between slow isometric contraction and relaxation. J. Physiol. 359, 107–118. https://doi.org/10.1113/jphysiol.1985.sp015577.

DeVries, H.A., 1968. EFFICIENCY OF ELECTRICAL ACTIVITY" AS A PHYSIOLOGICAL MEASURE OF THE FUNCTIONAL STATE OF MUSCLE TISSUE. Am. J. Phys. Med. 47, 10–22.

dos Anjos, F.V., Pinto, T.P., Cerone, G.L., Gazzoni, M., Vieira, T.M., 2022. Is the attenuation effect on the ankle muscles activity from the EMG biofeedback generalized to – or compensated by – other lower limb muscles during standing? J. Electromyogr. Kinesiol. 67, 102721.

Duchateau, J., Enoka, R.M., 2008. Neural control of shortening and lengthening contractions: influence of task constraints. J. Physiol. 586, 5853–5864. https://doi.org/10.1113/jphysiol.2008.160747.

Ekblom, M.M., Eriksson, M., 2012. Concurrent EMG feedback acutely improves strength and muscle activation. Eur. J. Appl. Physiol. 112, 1899–1905. https://doi.org/10.1007/s00421-011-2162-2.

Frigon, A., Thompson, C.K., Johnson, M.D., Manuel, M., Hornby, T.G., Heckman, C.J., 2011. Extra Forces Evoked during Electrical Stimulation of the Muscle or Its Nerve Are Generated and Modulated by a Length-Dependent Intrinsic Property of Muscle in Humans and Cats. J. Neurosci. 31 (15), 5579–5588.

Fukuhara, S., Kawashima, T., Oka, H., 2021. Indices reflecting muscle contraction performance during exercise based on a combined electromyography and mechanomyography approach. Sci. Rep. 11, 1–9. https://doi.org/10.1038/s41598-021-00671-2.

Grosprêtre, S., Gimenez, P., Martin, A., 2018. Neuromuscular and electromechanical properties of ultra-power athletes: the traceurs. Eur. J. Appl. Physiol. 118, 1361–1371. https://doi.org/10.1007/s00421-018-3868-1.

Jenz, S.T., Beauchamp, J.A., Gomes, M.M., Negro, F., Heckman, C.J., Pearcey, G.E.P., 2023. Estimates of persistent inward currents in lower limb motoneurons are larger in females than in males. J. Neurophysiol. 129, 1322–1333. https://doi.org/10.1152/jn.00043.2023.

Jesunathadas, M., Marmon, A.R., Gibb, J.M., Enoka, R.M., 2010. Recruitment and derecruitment characteristics of motor units in a hand muscle of young and old adults. J. Appl. Physiol. 108, 1659–1667. https://doi.org/10.1152/japplphysiol.00807.2009.

Keenan, K.G., Collins, J.D., Massey, W.V., Walters, T.J., Gruszka, H.D., 2011. Coherence between surface electromyograms is influenced by electrode placement in hand muscles. J. Neurosci. Methods 195, 10–14. https://doi.org/10.1016/j.jneumeth.2010.10.018.

Kimura, T., Yamanaka, K., Nozaki, D., Nakazawa, K., Miyoshi, T., Akai, M., Ohtsuki, T., 2003. Hysteresis in corticospinal excitability during gradual muscle contraction and relaxation in humans. Exp. Brain Res. 152, 123–132. https://doi.org/10.1007/s00221-003-1518-1.

Kirnap, M., Calis, M., Turgut, A.O., Halici, M., Tuncel, M., 2005. The efficacy of EMG-biofeedback training on quadriceps muscle strength in patients after arthroscopic meniscectomy. N. z. Med. J. 118, 1–9.

Kuznetsova, A., Brockhoff, P.B., Christensen, R.H.B., 2017. lmerTest Package: Tests in Linear Mixed Effects Models. J. Stat. Softw. 82, 1–26. https://doi.org/10.18637/JSS.V082.I13.

Łochyński, D., Celichowski, J., 2009. Tetanic depression and catch-like effect in fast motor units of the rat medial gastrocnemius at linearly increasing and decreasing stimulation frequencies. J. Muscle Res. Cell Motil. 30, 153–160. https://doi.org/10.1007/s10974-009-9185-x.

Lozano-García, M., Estrada-Petrocelli, L., Torres, A., Rafferty, G.F., Moxham, J., Jolley, C.J., Jané, R., 2021. Noninvasive assessment of neuromechanical coupling and mechanical efficiency of parasternal intercostal muscle during inspiratory threshold loading. Sensors 21, 1–15. https://doi.org/10.3390/s21051781.

Mackay, E.J., Robey, N.J., Suprak, D.N., Buddhadev, H.H., San Juan, J.G., 2023. The effect of EMG biofeedback training on muscle activation in an impingement population. J. Electromyogr. Kinesiol. 70, 102772 https://doi.org/10.1016/j.jelekin.2023.102772.

McManus, L., Lowery, M., Merletti, R., Søgaard, K., Besomi, M., Clancy, E.A., van Dieën, J.H., Hug, F., Wrigley, T., Besier, T., Carson, R.G., Disselhorst-Klug, C., Enoka, R.M., Falla, D., Farina, D., Gandevia, S., Holobar, A., Kiernan, M.C., McGill, K., Perreault, E., Rothwell, J.C., Tucker, K., Hodges, P.W., 2021. Consensus for experimental design in electromyography (CEDE) project: Terminology matrix. J. Electromyogr. Kinesiol. 59, 102565.

Merletti, R., Cerone, G.L., 2020. Tutorial. Surface EMG detection, conditioning and pre-processing: Best practices. J. Electromyogr. Kinesiol. 54, 102440 https://doi.org/10.1016/j.jelekin.2020.102440.

Merletti, R., Muceli, S., 2019. Tutorial. Surface EMG detection in space and time: Best practices. J. Electromyogr. Kinesiol. 49, 102363 https://doi.org/10.1016/j.jelekin.2019.102363.

Milner-Brown, H.S., Stein, R.B., Yemm, R., 1973. Changes in firing rate of human motor units during linearly changing voluntary contractions. J. Physiol. 230, 371–390. https://doi.org/10.1113/jphysiol.1973.sp010193.

Moritani, T., DeVries, H.A., 1980. Potential for gross muscle hypertrophy in older men. Journals Gerontol. 35, 672–682. https://doi.org/10.1093/geronj/35.5.672.

Nielsen, J.L.G., Holmgaard, S., Ning Jiang, Englehart, K.B., Farina, D., Parker, P.A., 2011. Simultaneous and Proportional Force Estimation for Multifunction Myoelectric Prostheses Using Mirrored Bilateral Training. IEEE Trans. Biomed. Eng. 58 (3), 681–688.

Onushko, T., Baweja, H.S., Christou, E.A., 2013. Practice improves motor control in older adults by increasing the motor unit modulation from 13 to 30 Hz. J. Neurophysiol. 110, 2393–2401. https://doi.org/10.1152/jn.00345.2013.

Orizio, C., Esposito, F., Sansone, V., Parrinello, G., Meola, G., Veicsteinas, A., 1997. Muscle surface mechanical and electrical activities in myotonic dystrophy. Electromyogr. Clin. Neurophysiol. 37, 231–239.

Orizio, C., Baruzzi, E., Gaffurini, P., Diemont, B., Gobbo, M., 2010. Electromyogram and force fluctuation during different linearly varying isometric motor tasks. J. Electromyogr. Kinesiol. 20, 732–741. https://doi.org/10.1016/j.jelekin.2010.03.005.

Orizio, C., Celichowski, J., Toscani, F., Calabretto, C., Bissolotti, L., Gobbo, M., 2013. Extra-torque of human tibialis anterior during electrical stimulation with linearly varying frequency and amplitude trains. J. Electromyogr. Kinesiol. 23, 1375–1383. https://doi.org/10.1016/j.jelekin.2013.07.008.

Schieppati, M., Crenna, P., 1985. Excitability of reciprocal and recurrent inhibitory pathways after voluntary muscle relaxation in man. Exp. Brain Res. 59, 249–256. https://doi.org/10.1007/BF00230904.

Schieppati, M., Nardone, A., Musazzi, M., 1986. Modulation of the Hoffmann reflex by rapid muscle contraction or release. Hum. Neurobiol. 5, 59–66.

Seki, K., Narusawa, M., 1996. Firing rate modulation of human motor units in different muscles during isometric contraction with various forces. Brain Res. 719, 1–7. https://doi.org/10.1016/0006-8993(95)01432-2.

Staudenmann, D., Roeleveld, K., Stegeman, D.F., van Dieen, J.H., 2010. Methodological aspects of SEMG recordings for force estimation - A tutorial and review. J. Electromyogr. Kinesiol. 20, 375–387. https://doi.org/10.1016/j.jelekin.2009.08.005.

Torricelli, D., De Marchis, C., D'Avella, A., Nemati Tobaruela, D., Oliveira Barroso, F., Pons, J.L., 2020. Reorganization of Muscle Coordination Underlying Motor Learning in Cycling Tasks. Front. Bioeng. Biotechnol. https://doi.org/10.3389/fbioe.2020.00800.

Vieira, T.M., Botter, A., Muceli, S., Farina, D., 2017. Specificity of surface EMG recordings for gastrocnemius during upright standing. Sci. Rep. 7, 1–11. https://doi.org/10.1038/s41598-017-13369-1.

Vieira, T.M., Cerone, G.L., Botter, A., Watanabe, K., Vigotsky, A.D., 2023. The sensitivity of bipolar electromyograms to muscle excitation scales with the inter-electrode distance. IEEE Trans. Neural Syst. Rehabil. Eng. PP, 1. https://doi.org/10.1109/TNSRE.2023.3325132.

Vieira, T.M.M., Loram, I.D., Muceli, S., Merletti, R., Farina, D., 2011. Postural activation of the human medial gastrocnemius muscle: Are the muscle units spatially localised? J. Physiol. 589, 431–443. https://doi.org/10.1113/jphysiol.2010.201806.